Atmospheric Releases during the 2003 Glacier Wildfires: Mapping, Analysis and Modeling

Germana Manca, Guido Cervone*, Keith C. Clarke***

*Geography and Geoinformation Science Department, George Mason University, Fairfax, Va
** Department of Geography, University of California Santa Barbara, Santa Barbara, Ca

ABSTRACT

A combined GIS and remote sensing approach to map and model the large wildfires in the summer 2003 at Glacier National Park. Numerical simulations were performed using the Clarke cellular automaton fire model, and the fire extents were validated using remote sensing data from the MODIS instrument. The results show a good correlation between the predicted fires and the actual. In addition, remote sensing data from the MODIS and TOMS instruments are used to quantify the optical dimming of the atmosphere caused by the fires. Atmospheric dimming correlated both spatially and temporally with the amount of burned fuel computed by the Clarke model. The observed atmospheric dimming is correlated both spatially and temporally with the fire simulations. Such knowledge is crucial in order to build a coupled land-atmosphere fire model.

Index Terms— GIS, RS, Wildfire, Atmospheric Dimming, Crosstabulation matrix, Modelling

1. INTRODUCTION

Fire spread models assess the rate of spread of a wildfire over a surface, taking into account the chemical, physical, and geometrical characteristics of the fire terrain, and the temperature, humidity and wind characteristics of the atmosphere (J. Scott, R. Burgan 2005, M. Siljander 2009 Z. Zhang, H. Zhang, D. Zhou 2010). They compute the chemical and physical fluxes, and used them to determine the fire spread over the geographical domain (R. Rothermel 1972). While other approaches to fire geometry and the relation with wind speed and slope has been developed (H.E. Anderson, J. K. Brown 1988), Anderson's classic descriptive model defines the shape of the wildfire as prevalently elliptical. In the absence of wind and on a flat surface, the elliptical shape becomes circular. Further refinements of fire modeling have been developed, and the appropriateness of a model for a fire situation is determined by: model form, complexity, available input data, environmental conditions, computational resources, ability to calculate parameters easily estimated by fire fighters, and time availability.

This study utilizes the Clarke Cellular Automaton Fire Model (K.C. Clarke and others 1995). This model was tested for validity using data from California's Santa Cruz Mountains (K.C. Clarke and G. Olson 1966). Moreover the Cellular Automata Fire Model approach shows a strong self-affinity with fractal theory, and perfectly matched the pattern of the wildfire and the above mentioned chaos theory, allowing outlying spot fires and unburned perforations in the fire scars.

Forest fires are known for increasing the aerosols in the atmosphere, and these contaminants severely affect the Earth's environment (L. Bourcier and others, 2010). Aerosol particles such as smoke, ash and soot can affect the climate system by reflecting, absorbing and scattering radiation. As a result, aerosols play a role in both the cooling and warming of the Earth. The study of atmospheric emissions is also crucial to identify high risk areas of contamination harmful to human health (G. Cervone and others, 2008). The residence time of aerosol particles is as short as that of water vapor in the troposphere (B. Albriet and others 2010). This is related to the fact that aerosols from the atmosphere can be removed by precipitation processes. Because of the short lifetime, it is very difficult to continuously observe aerosol distributions. However with the advent of remote sensing, it is possible to monitor aerosol concentration in the atmosphere, and to study their interaction with natural and man made phenomena like forest fires (K. Barrett and others 2010) (M. Amraoui and others 2010).

One of the drawbacks of the proposed method is the inability of the model to assess the atmospheric effect of the fire. It is generally very hard to compute the amount of aerosols released in the atmosphere from fire burning, due to the many factors involved, such as the characteristics of the burning mass, the moisture content, temperature, wind characteristic, etc. With the eventual goal of developing a joint land-atmosphere fire model as a first step, we have investigated the relationship between burned area and atmospheric dimming as detected by remote sensing instruments. Using data from the NASA Moderate Resolution Imaging Spectroradiometer (MODIS) and the Total Ozone Mapping Spectrometer (TOMS) instruments, we have computed spatio-temporal statistics of the atmospheric dimming associated with the fire. In this research, we used a combined approach using a GIS-based

Figure 1. 2003 Forest Fires in the Glacier National Park observed by MODIS.

fire model and remote sensing data to simulate the progression of wildfires, and their atmospheric effects, that occurred in Glacier National Park during the summer of 2003. Several large fires occurred during mid July to mid September, burning about 125,400 hectares (Figure 1).

2. GLACIER NATIONAL PARK

Glacier National Park Figure 1 is located in the north of the state of Montana, covering an area of 405,000 hectares of forests, alpine meadows, and lakes. The park is adjacent to the Canadian Waterton Lakes National Park, and together they form the Waterton-Glacier International Peace Park. Glacier National Park is affected by an average of 15 fires each summer and has averaged 2000 hectares burned each year. Most fires are short in length, lasting less than two weeks. During the summer of 2003, Glacier National Park was affected by several large fires during mid July to mid September, which destroyed about 125,400 hectares. Such fires could be observed using spaceborne observations (http://www.gsfc.nasa.gov/topstory/2003/0729glacier.html) using the MODIS instrument onboard the TERRA satellite.

3. RESULTS

The control file used for this model application set up the following weather conditions: 7 wind direction (come from the north); 6 wind magnitude (scale from 1 to 7); 30 air temperature (degree Celsius); 20% relative humidity. A fire is ignited at a location given by the model user. A random number is then drawn to determine direction of movement. The new firelet location is then burned, and the fires move on. Each fire center continues to generate random fire "runs" of a length that reflects the fuel moisture and pre-heating conditions until its firelets find no unburned fuel. When successive runs find no new fuel to burn, this fire center goes out. The burned area is a place of 1.127 million tonnes of biomass. In the area considered, where the wildfire was most dangerous, the amount of burnt surface in the simulation was 98.87 square kilometers, while in the real instance, the fire burned 124.68 square kilometers. The rounded ratio between the real and the simulated fire extent is 80%, a 20% underestimate. Figure 2 shows the simulated and observed burned area. A first approach to identify generally the comparison between the two images, the real wildfires extension and the simulated, has been carried out through a statistic analysis. The results of this analysis are highlighted in the next table 1 (Statistic of individual layers: correlation matrix):

Layer	Real	Simulated
Real	1.00	0.66
Simulated	0.66	1.0

Table 1. Statistic of individual layers: the correlation matrix between the real and simulated wildfire extension.

The correlation matrix reports a value of high positive linear correlation. In this case the variable pair shows a concordance between the two layers. In order to determine with accuracy the behavior of the two layers, a further analysis is required. The approach is based on a map comparison. This is carried out, using the crosstabulation matrix, where the rows are classes of the comparison map and the columns are classes of the reference map. The analysis, applied to verify the correspondence of the two maps, is based on the composite operator, in which the assessment of the agreement is calculated through a diagonal entries and off-diagonal entries (R.G.Pontius and M.L. Cheuk 2006, R.G.Pontius and J. Connors 2009, R.G.Pontius and K. Kuzera 2008), applying soft-classification. The location of the pixel, inside the boundaries of the pixel, determines the agreement, if its position is on the diagonal, or disagreement, if it is outside. The crosstabulation matrix at the fine resolution reports the same results for the minimum, multiplication, and composite rules, and the overall agreement is 84,07%. Moving forward to the medium resolution the agreement still grows, at a low percentage, to reach 84,15% at the coarsest resolution. This behavior is justified by the meaning of the composite operator. It refers to the agreement within the boundaries of a pixel, consequently larger boundaries mean larger agreement. This result outlines the high correlation between the two matrices, and the overall agreement between the maps remains the same.
Although there is a very high degree of correspondence between the observed satellite data and the simulation results, there are both false positives (burned areas in the simulation but not in the observed data) and false negatives (burned areas in the observed data, but not in the simulation).
In order to study the atmospheric dimming associated with this large volume of biomass burning, an in depth analysis of the atmosphere's optical properties was performed using the NASA TOMS and MODIS instruments. Aerosol Optical Depth (AOD) data from MODIS (TERRA) level 3 atmospheric monthly product, generated by combining the daily mean of AOD at 0.55 microns for both ocean and land. The analysis is based on 46 months of data from March 2000 to December 2003 which were downloaded from the NASA EOS Gateway. The data covers the region bounded

by latitude 42N to 52N and longitude 103W to 120W, with resolution of 1° latitude and 1° longitude. MODIS data, available on a monthly basis, was paired with Aerosol Index (AI) data from the TOMS (EarthProbe) daily product.

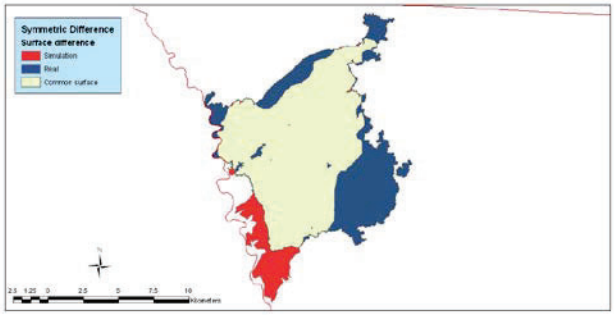

Figura 2. Comparison between simulated and observed burned area. Real area indicates false positive, while blue area, false negative. The green area is correct estimation by the model.

Figure 3 shows the sequence of AOD from July 2003 to October 2003. It 4 shows the AOD time series for 6 different locations of the Glacier National Park. In all graphs a strong seasonal effect is present, showing AOD oscillations from 0.5 during the winter months to 0.4 during the summer months. The AOD is notably high in July, August and September, reaching maximum values in August.

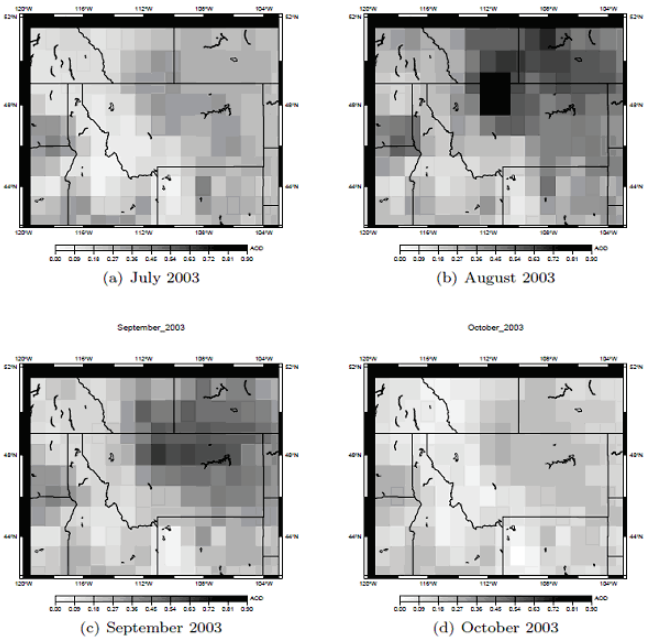

Figure 3. Aerosol Optical Depth for Summer 2003

In all graphs, a single prominent AOD peak as high as 0.9 is found in August 2003, which corresponds to the time and place of the forest fires. Such strong increase in the monthly data is due to the prolonged burning of forest which occurred in this region, leading to a large increase of the AOD. The lower mean values of July and September with respect to August are due to the presence of forest burning only in half of the months, because the largest fires were detected at the end of August.

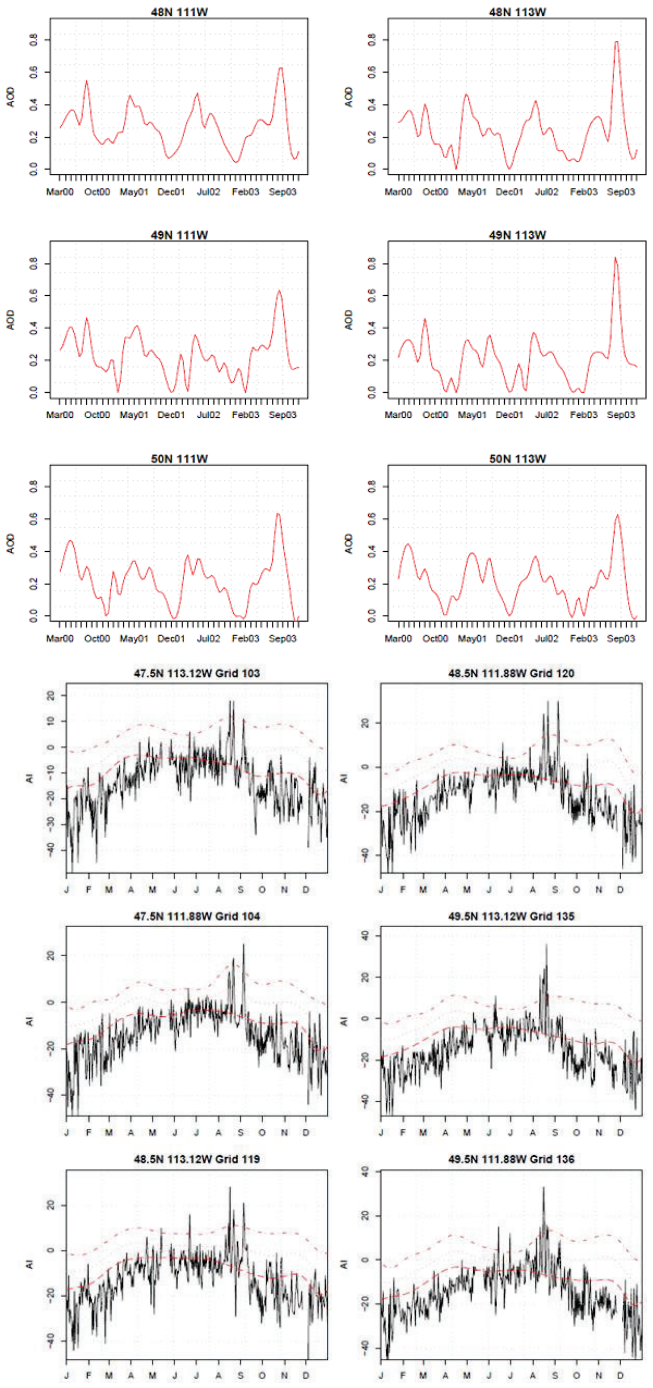

Figura 4. Time Series for several locations over the Glacier National Park using MODIS (up), and TOMS (down) data

Figure 4 (left) shows the AI time series for six location of the Glacier National Park. The locations for the time-series closely correspond to the locations in Figure 3. Figure 4 (right) shows the AI time-series for year 2003, its30-day average computed using data from 2000 to 2002 (3 years), and 1 and 2 standard deviation (sigma). The graphs

correspond to the locations of Figure 3. In all graphs there are prominent peaks, as high as 5 sigmas, during the months of July, August and September. These peaks are associated with the forest fires, and are consistent with the MODIS AOD increase. Values as high as 37 are recorded towards the end of August 2003. Such a prominent increase is due to the large amount of biomass burning.

Therefore the amount of atmospheric dimming caused by the fires corresponds to a 100% increase from .04 to .08 in AOD data. With respect to AI data, the maximum daily variation shows an increase of about 5 sigmas, with a peak of 37.

4. CONCLUSION

This paper presented an application of the Clarke fire model to the large 2003 forest fires of the Glacier national park. The model simulations were validated with land cover data from the MODIS instrument, and an agreement of more than 80% was observed. The crosstabulation matrix shows a high comparison between the simulated and real maps.

The geographical methodological approach copes with the capability to determine the discrepancy involving two geographical dataset, the real burnt area and the simulation output. This result is a collection of the manipulated dataset, the mentioned aforesaid images, where the geographical precision and the topological construction allow getting a related output of the burnt area.

Due to the model's inability to estimate atmospheric transport and dispersion of the smoke, we have analyzed the optical atmospheric dimming associated with the fires using data from MODIS and TOMS instruments. The large atmospheric dimming observed both spatially and temporally is associated with the biomass burning. In particular, we have observed a 100% increase in AOD values, and 500% increase in AI values. These results are encouraging in our goal of building an integrated fire-atmosphere coupled model.

5. REFERENCE

[1] J. Scott, R. Burgan, *Standard fire behavior fuel models: a comprehensive set for use with rothermel's surface fire spread model*, Tech. Rep. RMRS-GTR-153, U.S. Department of Agriculture, Forest Service, Rocky Mountain Research Station, 2005.

[2] M. Siljander, Predictive fire occurrence modelling to improve burned area estimation at a regional scale: A case study in east Caprivi, Namibia, *International Journal of Applied Earth Observation and Geoinformation,* 11 (6) 380–393, Dec. 2009.

[3] Z. Zhang, H. Zhang, D. Zhou, Using gis spatial analysis and logistic regression to predict the probabilities of human-caused grassland fires, *Journal of Arid Environments* 74 (3) 386–393, Mar. 2010.

[4] R. Rothermel, *A mathematical model for predicting fire spread in wildland fuels*, Tech. Rep. RP-INT-115, U.S. Department of Agriculture, Intermountain Forest and Range Experiment Station, 1972.

[5] H. E. Anderson, J. K. Brown, *Fuel characteristics and fire behavior considerations in the wildlands*. Symposium and workshop: protecting homes from wildfire in the interior west, Missoula, MT, 1987.

[6] M. A. Finney, *An overview of flammap fire modeling capabilities*, in: Fuels Management – How to measure success, Vol. I of P.L.Andrews, B.W. Butler (comps.), pp. 213–219, 2006.

[7] A. Bachmann, B. Allgöwer, Uncertainty propagation in wildland fire behaviour modelling, *International Journal of Geographical Information Science*, 16 (2), pp. 115–127, 2002.

[8] E. Pultar, M. Raubal, T. J. Cova, M. F. Goodchild, Dynamic GIS case studies: Wildfire evacuation and volunteered geographic information, *Transactions in GIS* 13 (s1), pp. 85–104, Jun. 2009.

[9] K.C. Clarke, P. Riggan,, J.A. Brass, A cellular automaton model of wildfire propagation and extinction, *Photogrammetric Engineering and Remote Sensing*, vol. 60, no. 11, pp. 1355-1367, 1995.

[10] K.C. Clarke, G. Olson, Refining a cellular automaton model of wildfire propagation and extinction, *GIS and Environmental Modeling: Progress and Research Issues*, GIS world books Edition, pp. 333–338, 1996.

[11] L. Bourcier, K. Sellegri, O. Masson, R. Zangrando, C. Barbante, A. Gambaro, J.-M. Pichon, J. Boulon, P. Laj, Experimental evidence of biomass burning as a source of atmospheric 137cs, puy de dˆome (1465 m a.s.l.), France, *Atmospheric Environment*, 44 (19), pp. 2280–2286, Jun. 2010.

[12] G. Cervone, P. Franzese, Y. Ezber, Z. Boybeyi, Risk assessment of atmospheric emissions using machine learning, *Natural Hazards and Earth System Science*, 8, pp. 991–1000, 2008.

[13] B. Albriet, K. Sartelet, S. Lacour, B. Carissimo, C. Seigneur, Modelling aerosol number distributions from a vehicle exhaust with an aerosol cfd model, *Atmospheric Environment*, 44 (8), pp. 1126–1137, 2010.

[14]. K. Barrett, E. Kasischke, A. McGuire, M. Turetsky, E. Kane, Modeling fire severity in black spruce stands in the alaskan boreal forest using spectral and non-spectral geospatial data, *Remote Sensing of Environment*, 114 (7), pp. 1494–1503, 2010.

[15] M. Amraoui, C. DaCamara, J. Pereira, Detection and monitoring of african vegetation fires using msg-seviri imagery, *Remote Sensing of Environment*, 114 (5), pp. 1038–1052, (2010).

[16] J.-L. Devineau, A. Fournier, S. Nignan, Savanna fire regimes assessment with modis fire data: Their relationship to land cover and plant species distribution in western Burkina Faso (West Africa), *Journal of Arid Environments*, 74 (9), pp. 1092–1101, 2010.

[17] R.G.Pontius, M.L. Cheuk, A generalized cross-tabulation matrix to compare soft-classified maps at multiple resolutions, *International Journal of Geographical Information Science*, 20 (1), pp. 1-30, Jan. 2006.

[18] R.G.Pontius, J. Connors, Range of categorical associations for comparison of maps with mixed pixels, *Photogrammetric Engineering & Remote Sensing,* 75(8), pp. 963-969, 2009.

[19] R.G.Pontius, K. Kuzera, Importance of matrix construction for multiple-resolution categorical map comparison, *GIScience & Remote Sensing*, 45(3), pp. 249-274, Aug. 2008.

[20] M.J.Kelty, A.W. D'Amato, P.K.Barten, Silvicultural and Ecological considerations of Forest Biomass Harvesting in Massachusetts, Manuscript prepared for Massachusetts Division of Energy Resources & Massachusetts Department of Conservation & Recreation, 2008.

[21] Takeyama, H. Couclelis, Map dynamics: integrating cellular automata and GIS thorugh GeoAlgebra, *International Journal of Geographical Information Science*, vol II, no. 1, 73-91, 1997.